ADA121237

Polytechnic Institute of New York

AFOSR-TR- 82-0890

HYPERSONIC AND OTHER VISCOUS INTERACTIONS

Robert J. Cresci and Martin H. Bloom

FINAL REPORT

October 1, 1980 - March 31, 1982

June 1982

POLY M/AE Report No. 82-10

Unclassified

SECURITY CLASSIFICATION OF THIS PAGE (When Data Entered)

REPORT DOCUMENTATION PAGE		READ INSTRUCTIONS BEFORE COMPLETING FORM
1. REPORT NUMBER AFOSR-TR- 82-0890	2. GOVT ACCESSION NO. AD-A121237	3. RECIPIENT'S CATALOG NUMBER
4. TITLE (and Subtitle) Hypersonic and Other Viscous Interactions		5. TYPE OF REPORT & PERIOD COVERED Final Report 1 Oct 80 - 31 Mar 82
		6. PERFORMING ORG. REPORT NUMBER
7. AUTHOR(s) Robert J. Cresci, Martin H. Bloom		8. CONTRACT OR GRANT NUMBER(s) AFOSR 81-0018
9. PERFORMING ORGANIZATION NAME AND ADDRESS Polytechnic Institute of New York, Route 110, Farmingdale, New York 11735		10. PROGRAM ELEMENT, PROJECT, TASK AREA & WORK UNIT NUMBERS 2307/A1 61102F
11. CONTROLLING OFFICE NAME AND ADDRESS Air Force Office of Scientific Research /NA, Building 410, Bolling AFB, DC 20332		12. REPORT DATE June 1982
		13. NUMBER OF PAGES 19
14. MONITORING AGENCY NAME & ADDRESS (if different from Controlling Office)		15. SECURITY CLASS. (of this report) Unclassified
		15a. DECLASSIFICATION/DOWNGRADING SCHEDULE

16. DISTRIBUTION STATEMENT (of this Report)

Approved for public release, distribution unlimited.

17. DISTRIBUTION STATEMENT (of the abstract entered in Block 20, if different from Report)

18. SUPPLEMENTARY NOTES

19. KEY WORDS (Continue on reverse side if necessary and identify by block number)

boundary layer transition
mass transfer
hypersonic flow

M (infinity)

20. ABSTRACT (Continue on reverse side if necessary and identify by block number)

Surface heat transfer and boundary layer transition measurements have been performed on a slender blunted cone at $M_\infty = 8.0$. These measurements have been obtained on the conical surface with mass transfer occurring on the spherical nose cap. The free stream Reynolds number, based on nose radius, varied between 0.6×10^4 and 0.9×10^5. Data was obtained both at zero angle of attack and at angles as high as 14°, which exceeds the semi-vortex

DD FORM 1 JAN 73 1473 EDITION OF 1 NOV 65 IS OBSOLETE

Unclassified

SECURITY CLASSIFICATION OF THIS PAGE (When Data Entered)

6000 90000

20. Abstract - Continued

cone angle of 10°. The technique utilized in the determination of transition location was a thin film gauge, on the model surface, which was maintained at a constant temperature by an anemometer system. The RMS output of the film gauge was found to accurately locate the onset of boundary layer transition.

A numerical analysis of film cooling in the stagnation region of a slender cone was also performed using the thin shock layer approximation. The porous region was analyzed and compared to previously obtained results using different assumptions. The downstream region, at angle of attack, utilize the porous region results as initial conditions. The computer program, however, was not successfully operated in this mode.

Grant No. AFOSR 81-0018,
Project 2307/A1

HYPERSONIC AND OTHER VISCOUS INTERACTIONS

Principal Investigators: Robert J. Cresci
Martin H. Bloom

FINAL REPORT

October 1, 1980 - March 31, 1982

Polytechnic Institute of New York
Aerodynamics Laboratories

June 1982

POLY M/AE Report No. 82-10

Summary

The studies performed under the sponsorship of this grant are both of an experimental and an analytical nature; these are summarized below:

(i) The experimental portion of the study involved the measurement of transition initiation on slender blunted cones in a hypersonic flow with mass transfer cooling. This was done for both zero and non-zero angle of attack conditions and included the development of a transition detection technique which utilized a thin surface film gauge. A correlation of $Re_{\theta_{tr}}$ was obtained which is useful in the prediction of transition under these conditions. The other aspect of the experimental program was the utilization of laser diagnostics to measure liquid water concentrations in a film cooled boundary layer. These programs are discussed in more detail in the following section.

(ii) The theoretical portion of the program centered on the numerical analysis of film cooling in the stagnation region of a slender cone, utilizing the thin shock layer approximation. The porous region was completely analzed and compared to previous analysis using different assumptions; this resulted in a technical publication. The downstream region was also analyzed and successfully tested at zero angle of attack. The angle of attack results would utilize the porous region results as initial conditions and are also expected to produce useful infor-

mation although the computer program was not tested in this mode.

The principal investigators on this grant for the period October 1980 through March 1982 were Prof. M. H. Bloom and Prof. R. J. Cresci.

List of Symbols

N_c	injection similarity parameter
P	pressure (lbs/ft^2)
R_o	nose radius (ft)
Re_∞	$\frac{\rho_\infty V_\infty R_o}{\mu_\infty}$ free stream Reynolds number
Re_θ	$\frac{\rho_e u_e \theta}{\mu_e}$ Reynolds number based on momentum thickness
s	downstream coordinate (ft)
T	temperature (°R)
t	time (sec)
V_∞	free stream velocity (ft/sec)
α	angle of attack (deg)
μ	viscosity coefficient ($lb\text{-}sec/ft^2$)
θ	momentum Thickness $\theta = \int_0^\infty \rho u(u_e - u)\,dy$
ϕ	transverse coordinate (deg)
ρ	density ($slugs/ft^3$)

Subscripts

c	coolant
e	boundary layer edge condition
tr	transitional

Superscripts

$-$	non-dimensional quantity
$\sim$	Lees transformed variable

TECHNICAL DISCUSSION

On slender bodies traveling at hypersonic speeds, whether mass is injected by an active coolant system or whether the injection occurs as a result of surface ablation, the major transfer of mass will occur in the stagnation region followed by a surface on which the effective injection rate is effectively zero. In the ablation system, this is caused by the radiation from the high temperature gases behind the bow shock wave in the nose-cap region. As the shock weakens in the downstream direction and becomes more conical in shape, the gas temperature drops rapidly and, along with it, the attendant surface ablation. If one considers the active coolant system, again one finds that the surface mass transfer is confined to the stagnation region since in this case the minimum injection required for reduction of convective heating is the important consideration. In either situation, however, there will be some residual cooling effect as the injected fluid flows downstream within the boundary layer.

It has been observed in ref. (1) that this increased boundary layer mass flow will initiate transition to turbulence earlier than in a boundary layer with no upstream injection. In a transitional or turbulent boundary layer, the local heat transfer is usually significantly higher than that in a laminar flow at the same free stream conditions. As a result, it is extremely important to be able to determine the onset of transition when such active cooling systems are proposed, or when they occur naturally through surface ablation. Downstream effects of mass injection on a slender cone were obtained in reference (2) from surface heat

transfer measurements; these measurements were then used to attempt to correlate the transition location with mass transfer rate and free stream Reynolds numbers. This is the only known previous study of transition located on the impermeable surface downstream of the mass transfer region.

The present study deals with a combined experimental and theoretical investigation of the downstream effects of mass transfer in the stagnation region of slender, conical bodies. Of particular interest is the transitional behavior of the boundary layer in the presence of upstream mass injection. Both zero and non-zero angles of attack were considered in both the experimental and theoretical portions of the study. Reference (3) describes both portions of the effort in a reasonably detailed fashion.

Experimental Studies

One purpose of the present study was to attempt to measure the onset of transition, on the impermeable surface, with greater accuracy than is possible by interpretation of surface heat transfer measurements. This was accomplished by using thin surface films which were heated and monitored by a constant temperature hot wire anemometer system. This technique was used to accurately locate the transition point under a variety of free stream Reynolds numbers, surface locations, and mass injection rates. The study was performed at a free stream Mach number of 8.0 on a spherically blunted cone of 10° half angle, as seen in figure (1); reference (4) describes this study in detail. Although the major portion of this study was conducted at zero angle of attack, some tests were run at angles of attack between 2° and 14°. Both the downstream

effectiveness and the transition location were also measured under these flow conditions. The tests were performed in a Mach 8.0 blow down wind tunnel, which has a two foot diameter, axisymmetric test section. The freestream stagnation temperature of the flow was maintained at 2000°R.; this is accomplished by heating the air in a pebble bed heater. The stagnation pressure of the air in the heater may be varied from 50 to 600 psia. The above stagnation conditions correspond to a range of freestream Reynolds numbers of 1.13×10^4 to 1.35×10^5 per inch.

Although surface heat transfer measurements were obtained in the current test program, the primary objective was to develop a technique which more accurately ascertained the transition location on the model. In the past, various methods have been utilized in the determination of transition location, e.g., surface heat transfer, Preston tubes, and thin film gauges. In the current test program it was decided to use the thin surface film technique, which utilizes standard TSI miniature flush mounted sensors in which the film is deposited on the end of a quartz cylinder 1.5mm in diameter. The gauge is maintained at a temperature slightly higher than that of the surrounding model by a constant temperature anemometer which is used to power the gauges and obtain the RMS sensor output.

The output of the anemometer, the RMS meter, the thermocouples and the pressure transducers was fed into a bank of Honeywell Accudata 122 linear amplifiers. The amplifiers normalized all incoming signals to a range of 0.0 to 1.0 volts. This normalized output was recorded on a Honeywell Model 101 AM-FM magnetic tape recorder. The microprocessor of the Model 101 can mark each

channel with a timing pulse so that all recorded data may be correlated in real time.

After the wind tunnel test run is terminated, the data recorded on the tape recorder is played back into a Digital PDP11-34 computer which has an AR-11 laboratory peripheral system. The AR-11 system is capable of analog to digital conversion of 16 channels of analog data, which is stored by the PDP11-34 on a diskette and is then ready for processing and analysis.

In order to obtain transition identification in a single test run, the free stream test Reynolds number was held constant while the mass transfer rate was varied. The results of a typical test are shown in figure (2), which presents the coolant chamber pressure vs. time and the RMS signal vs. time at a surface location of $\bar{s} = 36.8$ and a free stream Reynolds number of 4.0×10^4. The location of transition is clearly evident on the RMS plot and determines the injected mass transfer rate required to initiate transition at the specified surface location and at the test Reynolds number chosen.

These data were correlated for a wide range of surface locations, Reynolds numbers and mass transfer rates. The results of this correlation are shown in figure (3) in which all the data are seen to follow the same trend in terms of the transitional Reynolds number based on momentum thickness.

One of the more interesting results of these tests was that transitional flow was observed close to the injection region, followed by a region of laminar flow which in turn was followed by another region of transitional and ultimately turbulent boundary

layer. This behavior occurred only at certain Reynolds numbers and implied a local relaminarization of the boundary layer. Figure (4) presents the mass transfer required to obtain transition as a function of surface location and free stream Reynolds number. The data obtained at the lower Reynolds number is what is typically expected, however, at $Re_\infty = 0.4 \times 10^5$ one may observe a transition reversal that occurs at values of $\bar{s}$ less than 25.

At angle of attack, the surface film gauge used to detect boundary layer transition was only run at the $\bar{s} = 9.09$ location. This data is shown in figure (5) for three meridian planes: windward ($\phi = 0$) cross plane ($\phi = 90°$), and one intermediate plane ($\phi = 60°$).

Some general conclusions can be reached from this test program and may be summarized as follows:

(i) An accurate determination of the transition location may be obtained by using thin surface film gauges, operated by a constant temperature anemometer system, by examination of the RMS signal.

(ii) A correlation of transition Reynolds numbers, based on momentum thickness, has been obtained in terms of the surface location and the mass transfer required to initiate transition.

(iii) For a certain range of free stream Reynolds numbers, the effect of mass transfer was to initiate early transition, followed by a region in which relaminarization of the boundary layer occurred.

(iv) Both surface heat transfer and transition data were obtained up to angles of attack greater than the half

cone angle. Reasonable mass injection rates were found to effectively reduce the nose-tip heat transfer to values which exist on the downstream conical surface, even at the highest angles of attack considered.

(v) On the windward meridian, the presence of non-zero angle of attack delayed boundary layer transition, even in the presence of the destabilizing mass transfer.

Theoretical Studies

Reference (5) presents a special case of the more generalized equations developed in reference (3). For this analysis a limiting form of the full axisymmetric shock layer equations is solved in the stagnation region. The limiting form of the equations ignores the elliptic nature of the more general equations and is equivalent to assuming local similarity. The streamwise momentum and continuity equations are evaluated using the coupled block tridiagonal algorithm. Energy is solved uncoupled from the rest of the system; the influence of temperature is less critical, as the characteristic shape of the velocity profiles is governed by the streamwise momentum and continuity equations. A variable grid is employed that ensures maximum resolution about the viscous interface.

Solutions to the system of equations have been found for a range of free-stream Mach numbers, Reynolds numbers, and injection rates up to 250% of the free-stream mass flux per unit area. The largest injection rates available in the literature appear to approach 80% of the free-stream mass flux. Zero-injection solutions for the present analysis are also presented in order to show the

range and consistency of the approximations. At low and moderate injection rates, comparisons with experimental data and alternative theories are given for profiles, standoff distance, and interface location. Effects of grid size are discussed. Comparisons of stagnation region profiles with downstream profiles are discussed, as is utilization of the solution as initial conditions for more complete numerical analyses, which could determine the downstream effects of large localized upstream injection.

The following conclusions may be obtained regarding this study: at low injection rates, solutions compare well with a variety of previous theories and experimental data. For very large injection rates the static pressure variation is significant and must be taken into account. Even at high injection rates and large Reynolds numbers good resolution can be achieved with a moderate number of points if the equations are cast in conservation form and streamwise momentum and continuity are solved as a coupled system. The number of iterations necessary for convergence varied from 12 for the zero-injection case at low Reynolds numbers to 35 for the injection case at high Reynolds numbers. This is not excessive considering the very large gradients involved in the viscous interface.

The solutions are ideally suited as initial conditions for marching techniques. Any downstream influence on the stagnation solution may be removed by global iteration. The algorithm can be easily applied, is stable, and handles large gradients without difficulty. Downstream profiles compare well with the stagnation solution in nondimensional shock layer coordinates. Keeping this in mind, it might be possible to initialize a time-dependent tech-

nique, which requires initial values for the entire flow field, knowing only the stagnation region solution.

This analysis was developed to generate initial conditions for a more complete three-dimensional analysis of the downstream effect of large localized upstream injection on hypersonic blunt bodies.

The downstream region of interest in the overall program was also treated by a numerical analysis of the shock layer equations. This analysis was set up to include both zero and non-zero angles of attack. The principal purpose of the analysis was to develop a numerical solution to the shock layer equations reflecting the effects of large upstream injection. To deal with the severe gradients characteristic of large mass injection, numerical techniques are utilized which have been shown to be capable of computing difficult flow problems. An unconditionally stable block-tridiagonal algorithm provides a coupled solution of the continuity, streamwise momentum, and transverse momentum equations. A modified central space difference equation is used for all convective transverse first derivatives of the transverse velocity to insure the unconditional stability of the algorithm. The energy equation is solved uncoupled from the rest of the system by a two-dimensional strongly implicit algorithm, which is capable of updating the solution to the energy equation in the entire transverse plane in one sweep. These techniques require somewhat more computer storage, however, they provide the necessary coupling of the boundary conditions and the dependent variables for a high degree of efficiency and rapid convergence rates.

To provide the upstream mass injection a porous injection

region subtending a spherical solid angle of 60° is located at the apex of the sphere-cone configuration (fig. 1). At present no provision for cross flow separation is incorporated into the analysis. Initial conditions are provided for angle of attack cases, by solving the fully viscous shock layer equations at an axisymmetric stagnation point for large rates of injection. The stagnation solution is then rotated to a body fixed coordinate system to initialize the three dimensional solution. The method requires no initial guess for the entire shock shape. The only assumption made on the shock is when the stagnation region initial profiles are computed, otherwise the shock shape is predicted at each step in the computation. The Rankine-Hugoniot conditions are used to compute the outer boundary conditions on the shock layer. The sphere cone interface is treated as a discontinuity in curvature, therefore, no differences in the flow variables are taken across the sphere-cone juncture. Provision is made in all the difference equations for variable grids in all coordinate directions. This is important in this case for the mass injection is abruptly terminated at a particular downstream location. The streamwise grid spacing at the injection cut off point must be fine enough to handle the streamwise transition from injection profiles to non-injection profiles. At this location discontinuities in surface heat transfer and shear stress have been found to occur.

It is realized that choosing the three dimensional coupled algorithm to solve the two momentum equations and the continuity equation, as well as choosing the strongly implicit plane algorithm to solve the energy equation requires more computer storage

than a local cascading scheme. This increase in computer storage is outweighed by the stability of the methods, the reduction in the number of iterations, the amount of grid points necessary and a possible increase in the accuracy of the solution.

The details of this analysis are described more fully in reference (3), however, no numerical results were available for the angle of attack condition. Computer operating difficulties and the possiblity of undiscovered bugs in the program prevented the successful operation of the program prior to the expiration of the grant.

Laser Diagnostics

The development of an optical, nonintrusive flow diagnostic system using laser Raman scattering techniques has also been underway to determine water vapor and liquid droplet concentrations in a high speed boundary layer. The presence of the water originates when a liquid film is utilized for nose tip cooling. As the film progresses downstream, it breaks up into droplets (or vaporizes) and it is therefore important to know the particular state of the water at any location in order to be able to evaluate the physical mechanism of film deterioration. In its original form, the system was based on the continuous wave, low level, coherent anti-Stokes Raman Scattering (CARS) arrangement. This system employing two argon-ion lasers had to be abandoned due to the nonreliability of the lasers supplied to us by the Control Laser Corp. of Orlando, Florida. A new laser system which became available to us recently has therefore been utilized for the development of a reliable CARS system to measure water vapour concentrations. Results have been obtained by this sytem which is

capable of resolving relatively minor concentrations of water vapour.

An effort was made to obtain the same results for liquid water as for the vapour in the laboratory using the same laser system. Normally, this would require either additional tests or another laser system, however, an attempt was made to obtain the concentrations of liquid water and water vapour simultaneously using only one laser. This system would allow one to determine the complete phase balance of the coolant at any instant of time, or at any location along the surface.

As part of the development of the laser diagnostic system for the simultaneous acquisition of concentration of water vapour and liquid water droplets, it has been possible to obtain both with the same laser, using separate CARS systems. This process utilizing the single Neodynium Yag laser and the appropriate specially designed tunable dye laser, derived from and pumped by a fraction of the main laser power, has been halted due to the lack of time. It is, however, believed that the approach is fundamentally sound and should be pursued in the future.

REFERENCES

(1) Cresci, R.J. and Libby, P.A.: "The Downstream Influence of Mass Transfer at the Nose of a Slender Cone". J. Aero. Sci. 29, 7, 1962.

(2) Starkenberg, J. and Cresci, R.J.: Boundary Layer Transition on a Film-Cooled Slender Cone. AIAA J. 14, 4, April 1976.

(3) Plostins, P.: A Theoretical and Experimental Investigation of the Hypersonic Viscous Shock Layer for Large Rates of Injection. Ph.D. Dissertation (Adviser: R. J. Cresci), June 1981.

(4) Plostins, P. and Cresci, R.J.: Effects of Mass Transfer on Transition Behavior at High Speeds. Poly M/AE Report No. 82-9, June 1982.

(5) Plostins, P. and Rubin, S.G.: The Axisymmetric Stagnation Region Full Shock Layer for Large Rates of Injection. Numerical Heat Transfer, vol. 4, 1981.

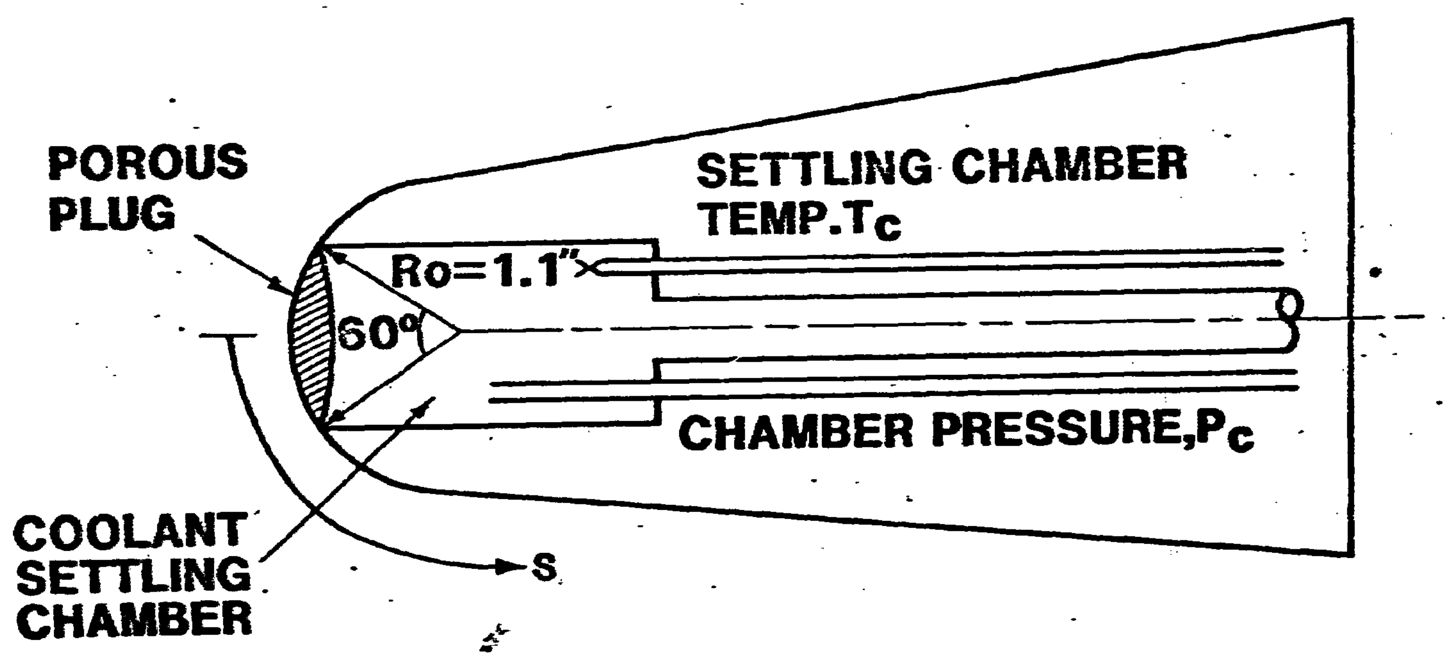

$\bar{S}$	1.36	1.82	2.27	2.95	3.64	4.32	5.45	6.96	8.47	9.09	14.66	25.0	36.8	47.0
T/C	X	X	X	X	X	X	X	X	X	X		X	X	X
FILM	X	X	X	X	X	X				X	X	X	X	X

FIG 1 MODEL SCHEMATIC

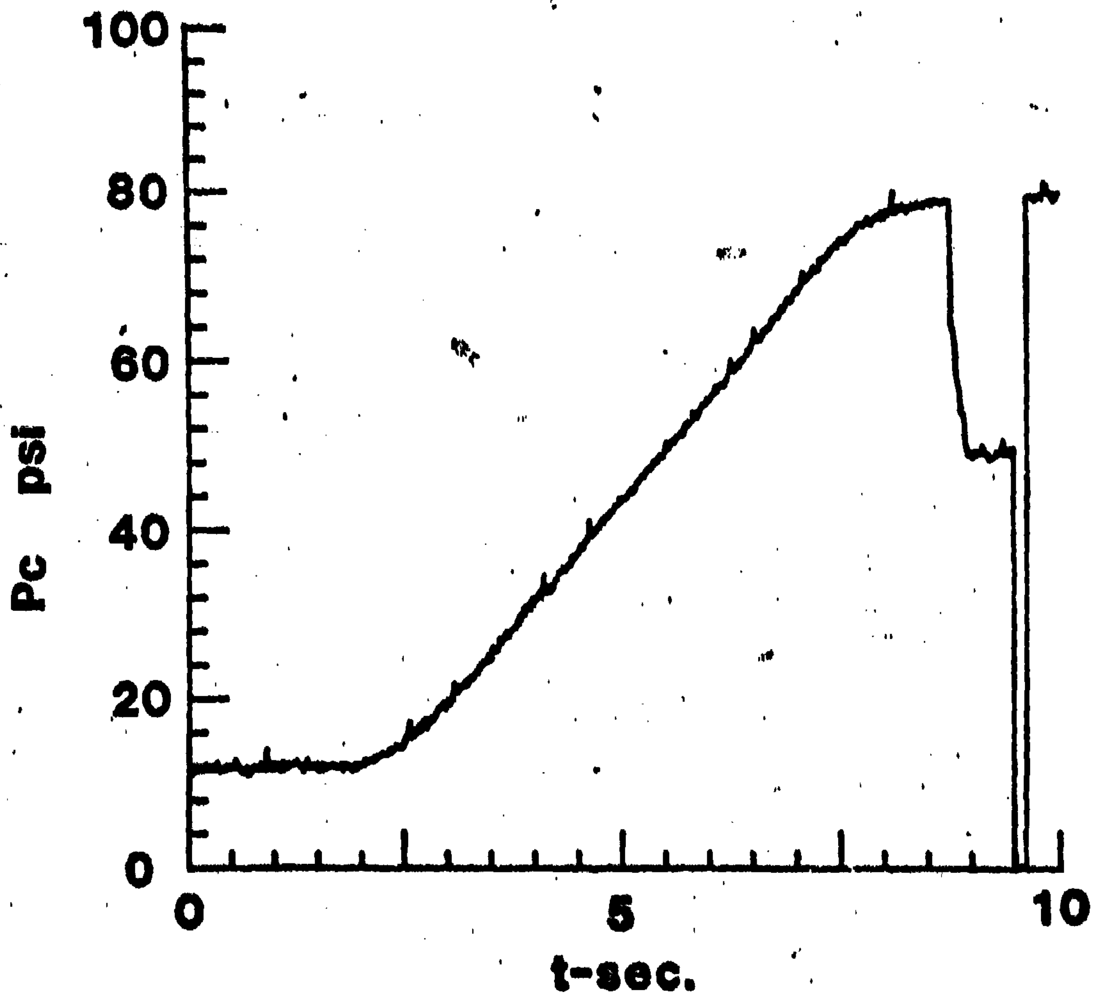

(a) CHAMBER PRESSURE

FIG 2 VARIABLE MASS FLOW $\bar{S}=36.8$

$Re_{\infty}=4.0\times10^4$ Ro=0.5IN. $\alpha=0°$

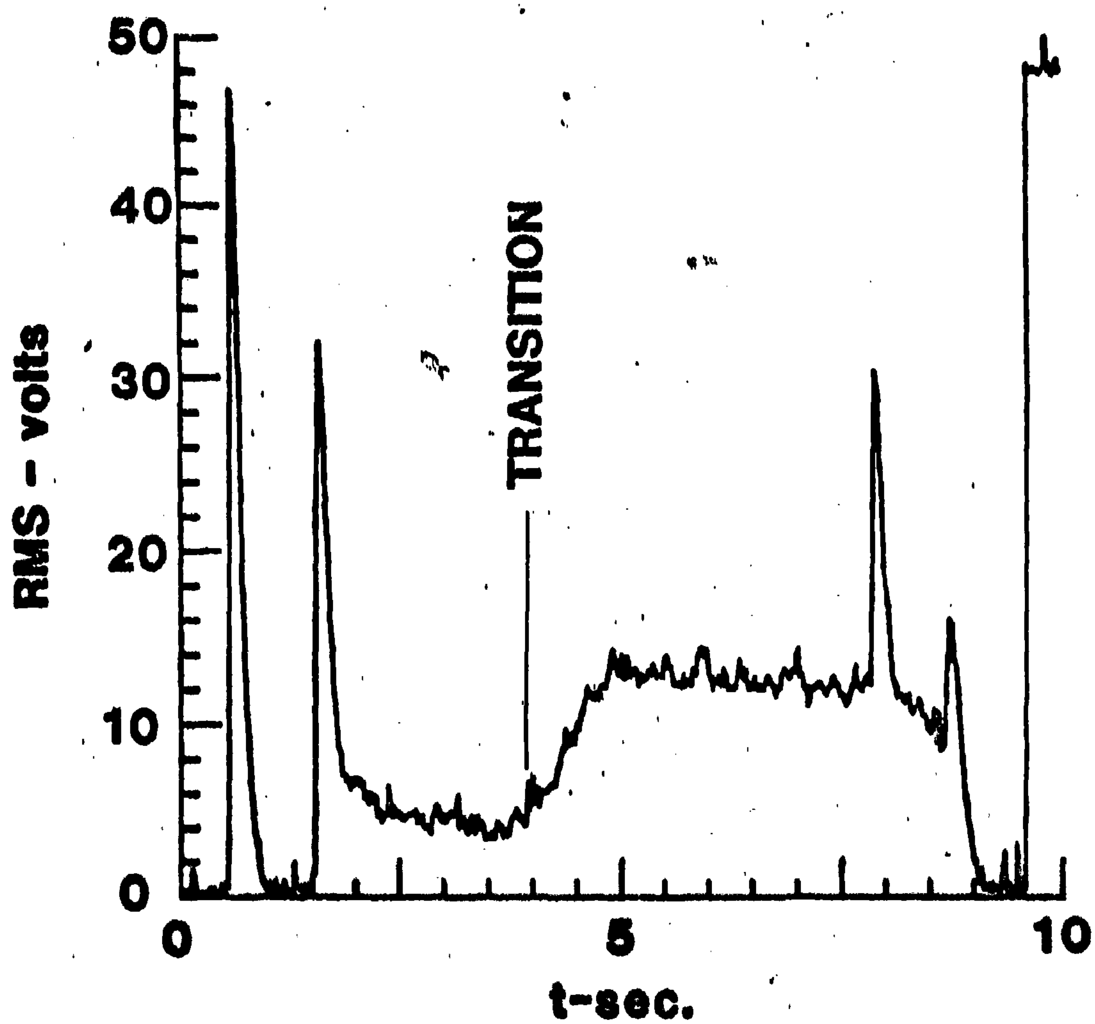

(b) RMS SIGNAL

FIG 2 VARIABLE MASS FLOW $\bar{S}=36.8$

$Re_{\infty}=4.0\times10^{4}$ Ro=0.5IN. $\alpha=0°$

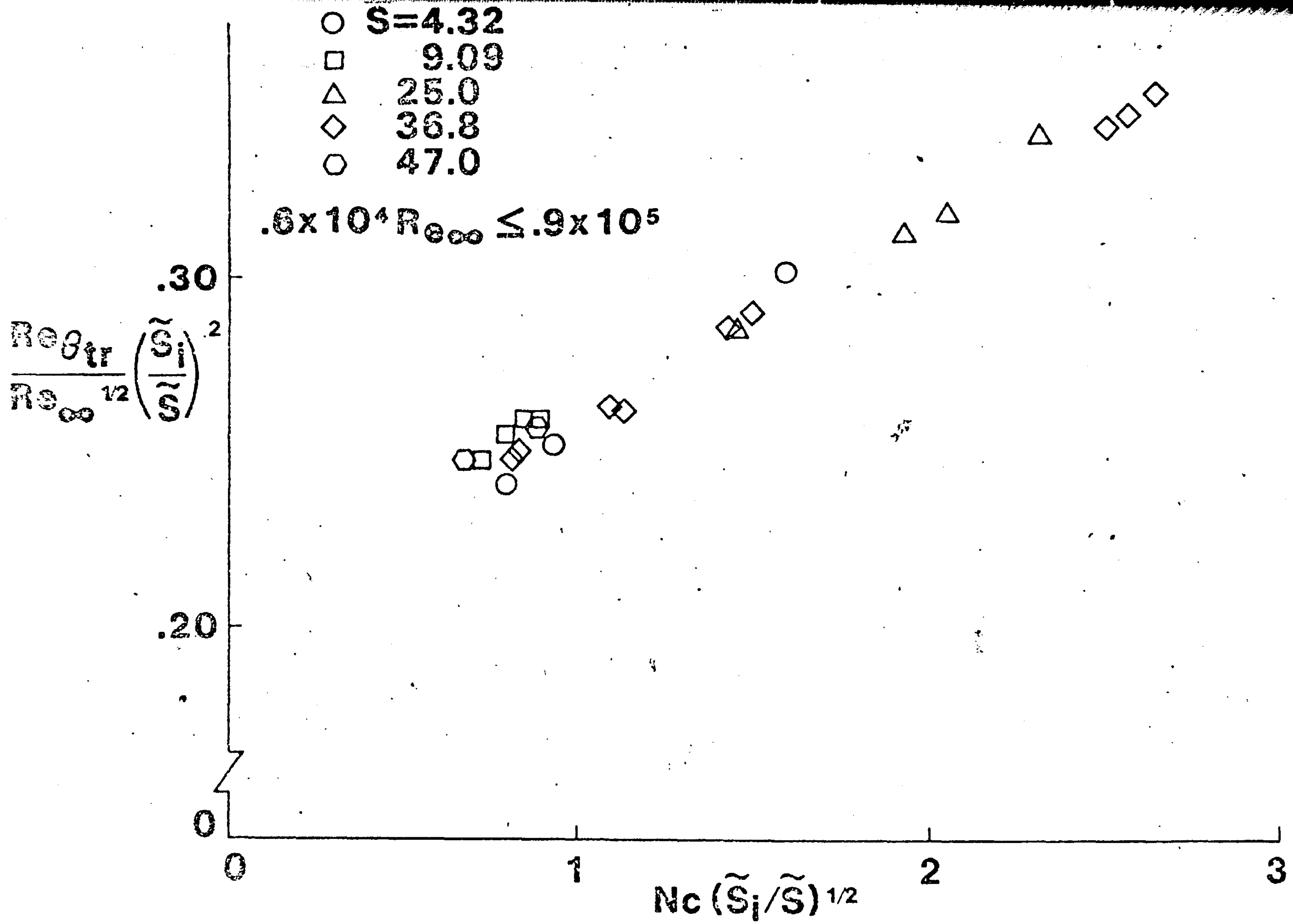

FIG 3 CORRELATION OF TRANSITIONAL Re_θ WITH MASS TRANSFER

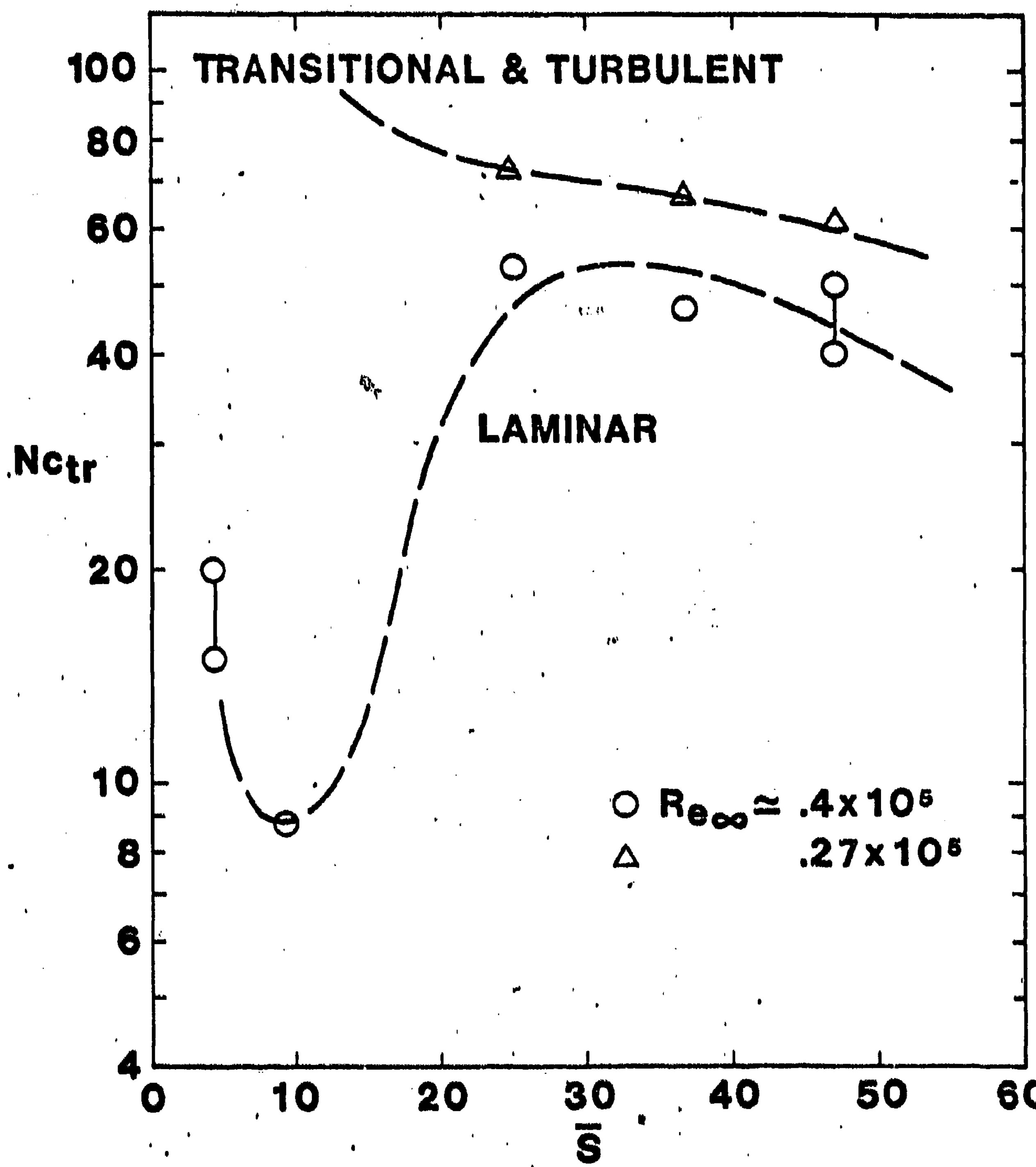

FIG 4 BOUNDARY LAYER RELAMINARIZATION

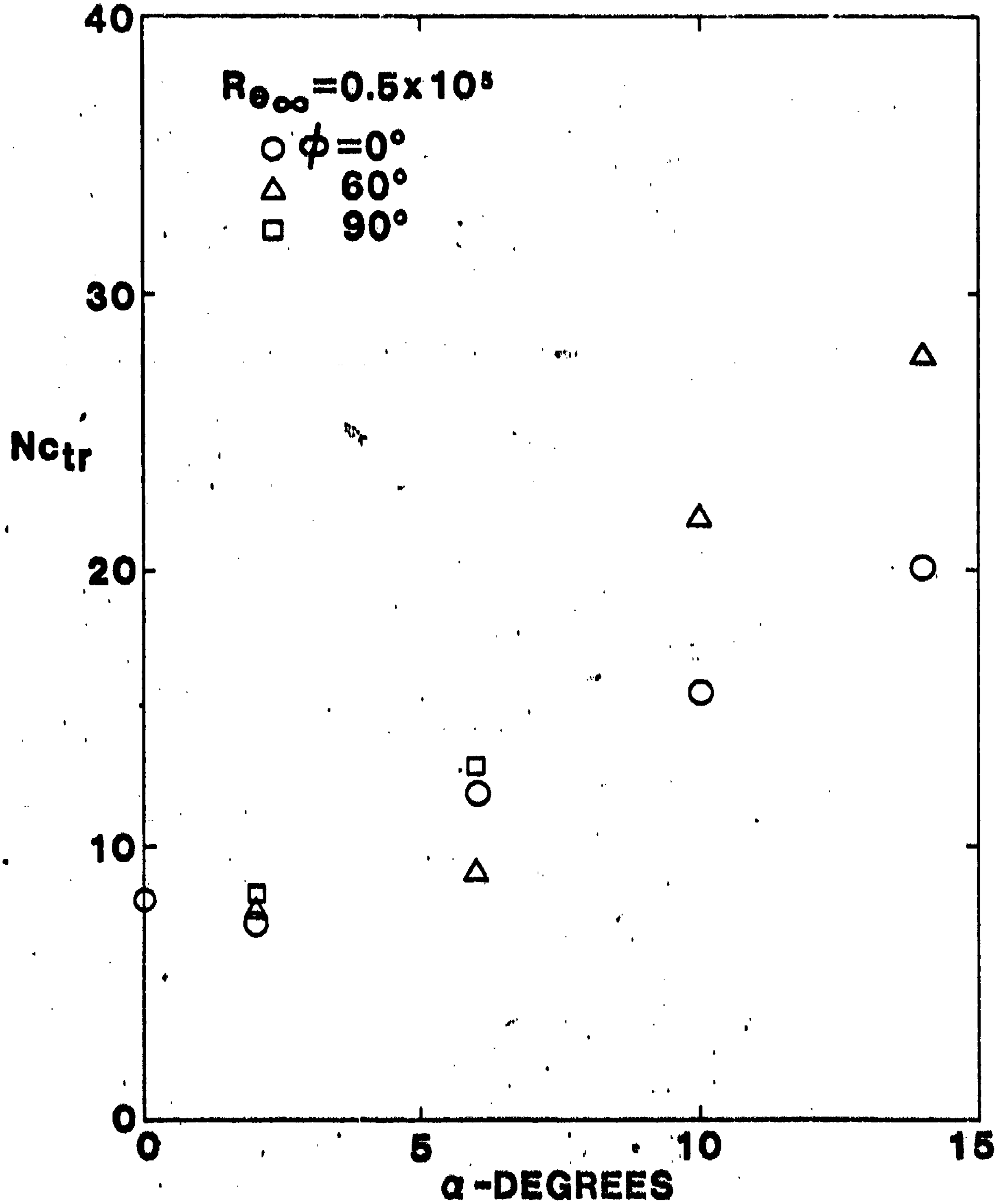

FIG 5 TRANSITIONAL BEHAVIOR at $\bar{S}=9.09$ vs. ANGLE OF ATTACK